Candidate multiple chiral doublets nucleus ^{106}Rh in a triaxial relativistic mean-field approach with time-odd fields

J. M. Yao (尧江明),[1] B. Qi (亓斌),[1] S. Q. Zhang (张双全),[1] J. Peng (彭婧),[2] S. Y. Wang (王守宇),[3] and J. Meng (孟杰)[1,4,5,6,*]

[1]*School of Phyics and State Key Laboratory of Nuclear Physics and Technology, Peking University, 100871 Beijing, People's Republic of China*

[2]*Department of Physics, Beijing Normal University, 100875 Beijing, People's Republic of China*

[3]*Department of Space Science and Applied Physics, Shandong University at Weihai, 264209 Weihai, People's Republic of China*

[4]*Institute of Theoretical Physics, Chinese Academy of Sciences, Beijing, People's Republic of China*

[5]*Center of Theoretical Nuclear Physics, National Laboratory of Heavy Ion Accelerator, 730000 Lanzhou, People's Republic of China*

[6]*Department of Physics, University of Stellenbosch, Stellenbosch, South Africa*

(Received 17 March 2009; published 9 June 2009)

The configuration-fixed constrained triaxial relativistic mean-field approach is extended by including time-odd fields and applied to the study of the candidate multiple chiral doublets (MχD) nucleus ^{106}Rh. The energy contribution from time-odd fields and microscopical evaluation of center-of-mass correction as well as the modification of triaxial deformation parameters β, γ due to the time-odd fields are investigated. The contributions of the time-odd fields to the total energy are 0.1–0.3 MeV, and they modify slightly the β, γ values. However, the previously predicted multiple chiral doublets still exist.

DOI: 10.1103/PhysRevC.79.067302 PACS number(s): 21.10.Dr, 21.60.Jz, 21.30.Fe, 27.60.+j

Since the prediction of the existence of chirality in atomic nuclei in 1997 [1] and later experimental observation of chiral doublet bands in 2001 [2], nuclear chirality has become one of the most interesting subjects in nuclear physics. Hitherto, extensive studies have been performed to understand the phenomena and explore their possible existence in $A \sim 100$, 130, and 190 mass regions [3–7].

On the theoretical side, chiral doublet bands were first predicted by the particle-rotor model (PRM) and tilted axis cranking (TAC) model for triaxially deformed nuclei [1]. Later on, numerous efforts were devoted to the development of TAC methods [8–11] and PRM models [12–15] to describe chiral rotation in atomic nuclei. It is shown that triaxial deformation and high-j valence particles and valence holes are essential for the formation of chirality in nuclei. Therefore, it will be very interesting to search for nuclei with these characters within the state-of-the-art nuclear structure models.

Relativistic mean-field (RMF) theory [16–20], which relies on basic ideas of effective field theory and density functional theory, has achieved great success in describing many nuclear phenomena for both stable and exotic nuclei over the entire nuclear chart. It thus provides us a microscopic way to study nuclear structure properties including the energy and deformation for not only the ground state but also the excited state for a given valence nucleon configuration. In Ref. [21], a configuration-fixed constrained triaxial RMF approach was developed and applied to study the nuclear potential energy surface (PES). An interesting phenomenon—the existence of multiple chiral doublets (MχD), i.e., more than one pair of chiral doublet bands in one single nucleus—has been suggested in ^{106}Rh and other odd-odd rhodium isotopes [22]. These predictions are based on the triaxial deformations of local minima and the corresponding proton and neutron configurations. In these studies, the time-reversal invariance was assumed from the beginning; that is, the time-odd fields were neglected.

Actually, the unpaired valence neutron and proton will generate nucleon currents and break the time-reversal invariance in a nuclear state. Such effects have been found to be of great importance in reproducing the nuclear magnetic moment [23] and inertia of moment [24] as well as the $M1$ transition rates in magnetic rotation nuclei [11]. Therefore one has to examine the existence of MχD in odd-odd rhodium isotopes with the presence of time-odd fields.

In this work, the configuration-fixed constrained triaxial RMF approach will be extended by including time-odd fields, which is more suitable to studying the triaxial structure properties of odd-mass and odd-odd nuclei. Taking ^{106}Rh as an example, the effect of time-odd fields on the total energy and triaxial deformations β, γ as well as on configuration will be examined.

The detailed description of the configuration-fixed constrained triaxial RMF approach with nucleon-nucleon interacting via meson exchange can be found in Ref. [21] and references therein. Only a brief outline, in particular with the presence of time-odd fields, will be given here.

The starting point of the RMF theory is the standard effective Lagrangian density constructed with the degrees of freedom associated with nucleon field (ψ), two isoscalar meson fields (σ and ω_μ), the isovector meson field ($\vec{\rho}_\mu$), and the photon field (A_μ). Under "mean-field" and "no-sea" approximations, one can derive the corresponding energy density functional, from which one finds immediately the equation of motion for a single-nucleon orbit $\psi_i(\boldsymbol{r})$ with the help of the variational principle

$$\{\alpha \cdot [\boldsymbol{p} - \boldsymbol{V}(\boldsymbol{r})] + \beta m^*(\boldsymbol{r}) + V_0(\boldsymbol{r})\}\psi_i(\boldsymbol{r}) = \epsilon_i \psi_i(\boldsymbol{r}), \quad (1)$$

*mengj@pku.edu.cn

where $m^*(\boldsymbol{r})$ is defined as $m^*(\boldsymbol{r}) \equiv m + g_\sigma \sigma(\boldsymbol{r})$, with m referring to the mass of the bare nucleon. The repulsive vector potential $V_0(\boldsymbol{r})$, i.e., the time-like component of vector potential, reads

$$V_0(\boldsymbol{r}) = g_\omega \omega_0(\boldsymbol{r}) + g_\rho \tau_3 \rho_0(\boldsymbol{r}) + e\frac{1-\tau_3}{2} A_0(\boldsymbol{r}), \quad (2)$$

where $g_i (i = \sigma, \omega, \rho)$ are the coupling strengths of the nucleon with mesons. The time-odd fields $\boldsymbol{V}(\boldsymbol{r})$ are naturally given by the space-like components of vector fields,

$$\boldsymbol{V}(\boldsymbol{r}) = g_\omega \boldsymbol{\omega}(\boldsymbol{r}) + g_\rho \tau_3 \boldsymbol{\rho}(\boldsymbol{r}) + e\frac{1-\tau_3}{2} \boldsymbol{A}(\boldsymbol{r}). \quad (3)$$

The nonvanishing time-odd fields in Eq. (3) give rise to splitting between pairwise time-reversal states $\psi_{\bar{i}}$ and $\psi_{\underline{i}}$ $(\equiv \hat{T}\psi_{\bar{i}})$, where $\hat{T}$ is the time-reversal operator. Each Dirac spinor $\psi_i(\boldsymbol{r})$ is expanded in terms of a set of three-dimensional harmonic oscillator (HO) bases in Cartesian coordinates with 12 major shells. The meson fields that provide the nuclear mean-field potentials are expanded in terms of the same HO basis as those of Dirac spinor but with 10 major shells. The pairing correlations are greatly quenched by the unpaired valence neutron and proton in ^{106}Rh and thus neglected. More details about the solution of the Dirac equation (1) with time-odd fields can be found in Ref. [25].

A configuration-fixed quadrupole moment constraint calculation through β^2 was carried out to obtain the PES for each configuration, where

$$\beta = \frac{4\pi}{3AR_0^2}\sqrt{q_{20}^2 + 2q_{22}^2}$$

and

$$\gamma = \tan^{-1}\left(\sqrt{2}\frac{q_{22}}{q_{20}}\right),$$

with

$$q_{20} = \sqrt{\frac{5}{16\pi}}\langle 2z^2 - x^2 - y^2\rangle$$

and

$$q_{22} = \sqrt{\frac{15}{32\pi}}\langle x^2 - y^2\rangle.$$

The same configuration is guaranteed during the procedure of the constraint calculation with the help of "parallel transport" [26], which enables one to decompose the whole PES into several parts characterized by the quantum numbers of corresponding configurations.

In Fig. 1, the energies are given as functions of deformation β in configuration-fixed constrained time-odd triaxial RMF calculations with PK1 set [27] for ^{106}Rh. The minima in the energy surfaces of each configuration are labeled with A, B, C, D, E, and F, respectively. The PES plotted with dashed line in Fig. 1 are obtained by the triaxial RMF calculation without time-odd fields. Furthermore, the center-of-mass (c.m.) correction energy is estimated phenomenologically with $E_{\text{c.m.}}^{\text{phe.}} = -\frac{3}{4} \times 41A^{-1/3}$, which remains to be a constant for all configurations. Here the c.m. correction energy is evaluated microscopically by projection-after-variation in the first-order approximation, i.e.,

$$E_{\text{c.m.}}^{\text{mic.}} = -\frac{1}{2mA}\langle \boldsymbol{P}_{\text{c.m.}}^2\rangle, \quad (4)$$

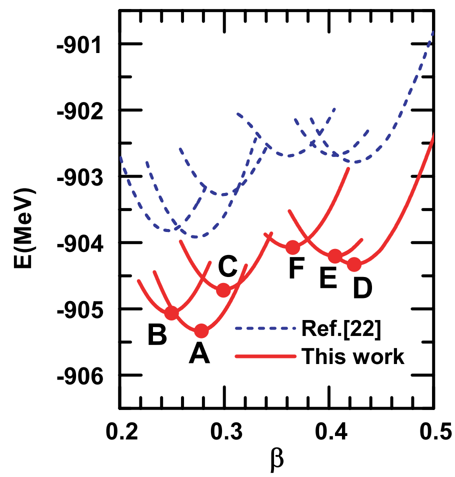

FIG. 1. (Color online) Potential energy surfaces as functions of deformation β in configuration-fixed constrained time-odd triaxial RMF calculations with PK1 set (solid line). The minima in the energy surfaces of each configuration are labeled A–F according to their energies. The results obtained without the time-odd fields (dashed line) are from Ref. [22].

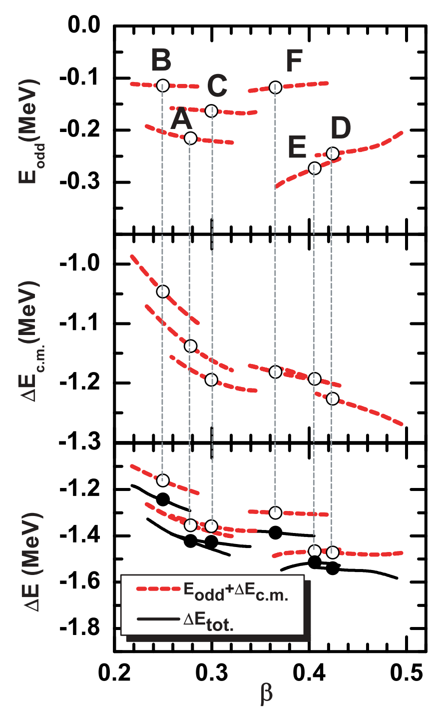

FIG. 2. (Color online) Energy from time-odd fields E_{odd} (upper panel), the energy difference between microscopic and phenomenological c.m. correction $\Delta E_{\text{c.m.}}$ (middle panel), and the summation of E_{odd} and $\Delta E_{\text{c.m.}}$ and the energy difference $\Delta E_{\text{tot.}}$ between the corresponding potential energy surfaces in Fig. 1 (lower panel) for different configurations as functions of deformation parameter β.

TABLE I. Total energies $E_{\rm tot.}$, center-of-mass correction energy $E_{\rm c.m.}$, energy contribution from the time-odd fields $E_{\rm odd}$, triaxial deformation parameters β, γ as well as their corresponding valence nucleon configurations for A–F in the configuration-fixed constrained triaxial RMF calculations with (without) time-odd fields. The values in parentheses are from Ref. [22].

State	Configuration	$E_{\rm tot.}$ (MeV)	$E_{\rm c.m.}$ (MeV)	$E_{\rm odd}$ (MeV)	β	γ
A	$\nu 2d^1_{5/2} \otimes \pi 1g^{-3}_{9/2}$	−905.33 (−903.92)	−7.64 (−6.50)	−0.22	0.28 (0.27)	24.3° (24.7°)
B	$\nu 1h^1_{11/2} \otimes \pi 1g^{-3}_{9/2}$	−905.06 (−903.82)	−7.55 (−6.50)	−0.11	0.25 (0.25)	23.1° (23.3°)
C	$\nu 1h^3_{11/2} \otimes \pi 1g^{-3}_{9/2}$	−904.72 (−903.28)	−7.69 (−6.50)	−0.16	0.30 (0.30)	22.4° (22.9°)
D	$\nu 1h^5_{11/2} \otimes \pi 2p^{-1}_{3/2}$	−904.33 (−902.79)	−7.73 (−6.50)	−0.25	0.42 (0.42)	3.9° (4.0°)
E	$\nu 1g^{-1}_{7/2} \otimes \pi 2p^{-1}_{3/2}$	−904.21 (−902.68)	−7.69 (−6.50)	−0.27	0.41 (0.41)	8.5° (8.8°)
F	$\nu 1g^{-1}_{7/2} \otimes \pi 1g^{1}_{7/2}$	−904.07 (−902.69)	−7.68 (−6.50)	−0.12	0.37 (0.36)	11.8° (11.9°)

where $\boldsymbol{P}_{\rm c.m.} = \sum_i^A \boldsymbol{p}_i$ and A is the mass number. It is found that the time-odd fields and microscopic c.m. correction do not change significantly the topological structure of the whole PES but lower it by about 1.5 MeV. As a result, the energy of the ground state is modified from −903.92 to −905.33 MeV, which is much closer to the experimental value of −906.72 MeV [28].

In Fig. 2, we plot the energy contribution from the time-odd fields $E_{\rm odd}\,[\equiv -\frac{g_\omega}{2}\int d^3\boldsymbol{r}\boldsymbol{\omega}(\boldsymbol{r})\cdot \mathbf{j}_N(\boldsymbol{r})$, with the nucleon current given by $\mathbf{j}_N = \sum_i \psi_i^\dagger \boldsymbol{\alpha}\psi_i]$, the c.m. correction energy difference $\Delta E_{\rm c.m.} = E^{\rm mic.}_{\rm c.m.} - E^{\rm phe.}_{\rm c.m.}$, and total energy difference $\Delta E_{\rm tot}$ between the present calculation and those in Ref. [22] as functions of deformation parameter β. All $E_{\rm odd}$, $\Delta E_{\rm c.m.}$, and $\Delta E_{\rm tot}$ change moderately as functions of β for a given configuration. Furthermore, the main contribution to $\Delta E_{\rm tot}$, i.e., the shift of whole PES in Fig. 1, is due to $\Delta E_{\rm c.m.}$. The time-odd fields make the nucleus more bound, and their contributions to the energy range around 0.1–0.3 MeV. The lower panel in Fig. 2 tells us that the time-odd fields will modify the time-even mean fields and lead to ∼0.1 MeV contribution to the total energy for all the configurations.

In Fig. 3, we plot the triaxial deformation parameters γ as functions of β in configuration-fixed constrained triaxial RMF calculations for ^{106}Rh without and with the time-odd fields.

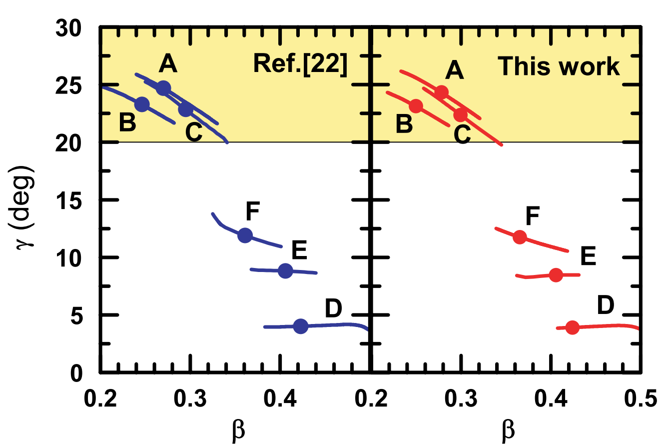

FIG. 3. (Color online) Triaxial deformation parameters γ as functions of β in configuration-fixed constrained triaxial RMF calculations for ^{106}Rh without (left) and with (right) the time-odd fields. The results in the left panel are from Ref. [22].

The shaded area represents the favorable triaxial deformation for chirality. It shows that triaxial deformation parameters β and γ are not sensitive to the time-odd fields. In both cases, the valence nucleon configurations A, B, and C have the favorable triaxial deformation for chirality.

To label the configuration A, B, and C, the main spherical component for the wave function of the valence nucleon was obtained by expanding the Dirac spinor in terms of the spherical HO basis with the quantum number $|nljm\rangle$. It is found that the influence of the time-odd fields for the composition of the Dirac spinor is negligible.

The total energies $E_{\rm tot.}$, center-of-mass correction energy $E_{\rm c.m.}$, energy contribution from the time-odd fields $E_{\rm odd}$, triaxial deformation parameters β, γ as well as their corresponding valence nucleon configurations for A–F in the configuration-fixed constrained triaxial RMF calculations with (without) time-odd fields are presented in Table I. It shows that the time-odd fields may reduce the triaxial deformation parameter γ by 0.5°. Using the structure information for the configuration $\nu h^1_{11/2} \otimes \pi g^{-3}_{9/2}$ as inputs in a triaxial rotor coupled with the quasiparticle model [14,15], the energy spectra and the electromagnetic transition ratios for a pair of negative-parity doublet bands in ^{106}Rh are well reproduced in Ref. [29].

In summary, the configuration-fixed constrained triaxial relativistic mean-field approach has been extended by including time-odd fields and applied to studying the candidate MχD nucleus ^{106}Rh. The energy contributions from time-odd fields and center-of-mass correction have been studied in detail. It has been found that the time-odd fields contribute 0.1–0.3 MeV to the total energy and slightly modify the triaxial deformation parameters β, γ. This confirms the previous prediction of the possible existence of MχD in the configuration-fixed triaxial RMF approach without time-odd fields. As one pair of doublet bands with $\nu h^1_{11/2} \otimes \pi g^{-3}_{9/2}$ configuration has been observed experimentally, it will be very interesting to search for the candidate chiral doublet bands with configuration $\nu h^3_{11/2} \otimes \pi g^{-3}_{9/2}$ and verify the prediction of MχD.

This work is partly supported by the National Natural Science Foundation of China under Grant Nos. 10775004, 10705004, 10875074, and 10505002, and the Major State Basic Research Development Program Under Contract No. 2007CB815000.

[1] S. Frauendorf and J. Meng, Nucl. Phys. **A617**, 131 (1997).
[2] K. Starosta *et al.*, Phys. Rev. Lett. **86**, 971 (2001).
[3] D. Tonev *et al.*, Phys. Rev. Lett. **96**, 052501 (2006).
[4] E. Grodner *et al.*, Phys. Rev. Lett. **97**, 172501 (2006).
[5] S. Mukhopadhyay *et al.*, Phys. Rev. Lett. **99**, 172501 (2007).
[6] P. Joshi *et al.*, Phys. Rev. Lett. **98**, 102501 (2007).
[7] J. Meng, B. Qi, S. Q. Zhang, and S. Y. Wang, Mod. Phys. Lett. A **23**, 2560 (2008), and references therein.
[8] V. I. Dimitrov, S. Frauendorf, and F. Donau, Phys. Rev. Lett. **84**, 5732 (2000).
[9] P. Olbratowski, J. Dobaczewski, J. Dudek, and W. Plociennik, Phys. Rev. Lett. **93**, 052501 (2004).
[10] P. Olbratowski, J. Dobaczewski, and J. Dudek, Phys. Rev. C **73**, 054308 (2006).
[11] J. Peng, J. Meng, P. Ring, and S. Q. Zhang, Phys. Rev. C **78**, 024313 (2008).
[12] J. Peng, J. Meng, and S. Q. Zhang, Phys. Rev. C **68**, 044324 (2003).
[13] T. Koike, K. Starosta, and I. Hamamoto, Phys. Rev. Lett. **93**, 172502 (2004).
[14] S. Y. Wang, S. Q. Zhang, B. Qi, and J. Meng, Phys. Rev. C **75**, 024309 (2007).
[15] S. Q. Zhang, B. Qi, S. Y. Wang, and J. Meng, Phys. Rev. C **75**, 044307 (2007).
[16] B. D. Serot and J. D. Walecka, Adv. Nucl. Phys. **16**, 1 (1986).
[17] P.-G. Reinhard, Rep. Prog. Phys. **52**, 439 (1989).
[18] P. Ring, Prog. Part. Nucl. Phys. **37**, 193 (1996).
[19] D. Vretenar, A. V. Afanasjev, G. A. Lalazissis, and P. Ring, Phys. Rep. **409**, 101 (2005).
[20] J. Meng, H. Toki, S.-G. Zhou, S. Q. Zhang, W. H. Long, and L. S. Geng, Prog. Part. Nucl. Phys. **57**, 470 (2006).
[21] J. Meng, J. Peng, S. Q. Zhang, and S.-G. Zhou, Phys. Rev. C **73**, 037303 (2006).
[22] J. Peng, H. Sagawa, S. Q. Zhang, J. M. Yao, Y. Zhang, and J. Meng, Phys. Rev. C **77**, 024309 (2008).
[23] U. Hofmann and P. Ring, Phys. Lett. **B214**, 307 (1988).
[24] J. Konig and P. Ring, Phys. Rev. Lett. **71**, 3079 (1993).
[25] J. M. Yao, H. Chen, and J. Meng, Phys. Rev. C **74**, 024307 (2006).
[26] R. Bengtsson and W. Nazarewicz, Z. Phys. A **334**, 269 (1989).
[27] W. Long, J. Meng, N. Van Giai, and S.-G. Zhou, Phys. Rev. C **69**, 034319 (2004).
[28] G. Audi, A. H. Wapstra, and C. Thibault, Nucl. Phys. **A729**, 337 (2003).
[29] S. Y. Wang, S. Q. Zhang, B. Qi, J. Peng, J. M. Yao, and J. Meng, Phys. Rev. C **77**, 034314 (2008).